Supplementary Information

Porous Macromolecular Dihydropyridyl Frameworks Exhibiting Catalytic and Halochromic Activity

Bo Xiao,[a,b] Timothy L. Easun,[a] Amarajothi Dhakshinamoorthy,[c,g] Izabela Cebula,[d,e] Peter H. Beton,[d] Jeremy J. Titman,[a] Hermenegildo Garcia,[c] K. Mark Thomas[f] and Martin Schröder*[,a]

[a] *School of Chemistry, University Park, University of Nottingham, Nottingham NG7 2RD, United Kingdom.*

[b] *School of Chemistry & Chemical Engineering, Queen´s University Belfast, David Keir Building, Stranmillis Road, Belfast BT9 5AG, United Kingdom.*

[c] *Instituto de Tecnología Química (CSIC-UPV), Avda. de los Naranjos s/n., 46022 Valencia, Spain.*

[d] *School of Physics and Astronomy University Park, University of Nottingham, Nottingham NG7 2RD, United Kingdom.*

[e] *Institute of Experimental Physics, University of Wroclaw, pl. M. Borna 9, 50-204 Wroclaw, Poland.*

[f] *Wolfson Northern Carbon Reduction Laboratories, School of Chemical Engineering and Advanced Materials, Newcastle University, Newcastle upon Tyne NE1 7RU, United Kingdom.*

[g] *Centre for Green Chemistry Processes, School of Chemistry, Madurai Kamaraj University, Tamil Nadu, India 625 021.*

(1) Spectroscopic Measurements

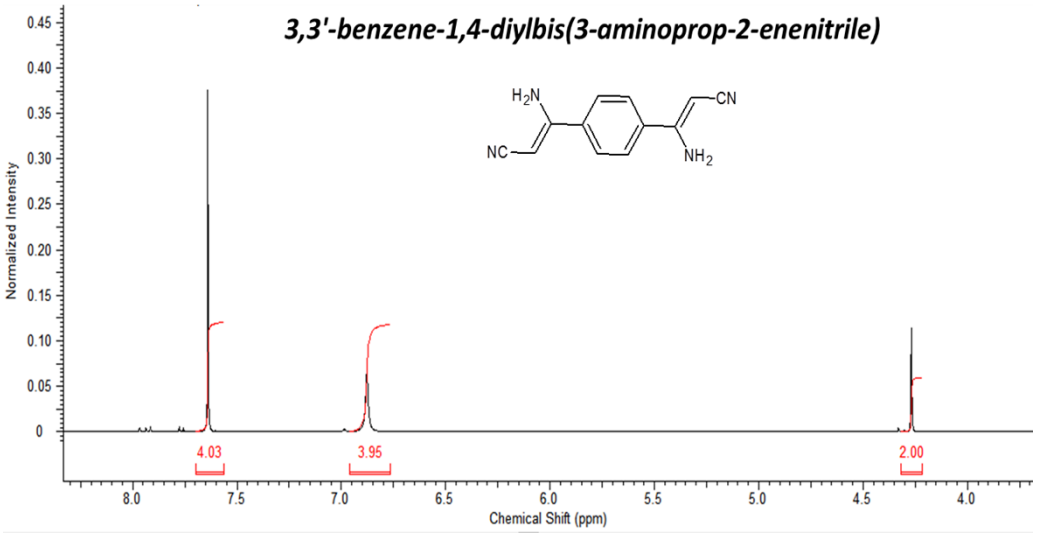

Figure S1. 1H-NMR (DMSO-d6) spectrum of 3,3'-benzene-1,4-diylbis(3-aminoprop-2-enenitrile).

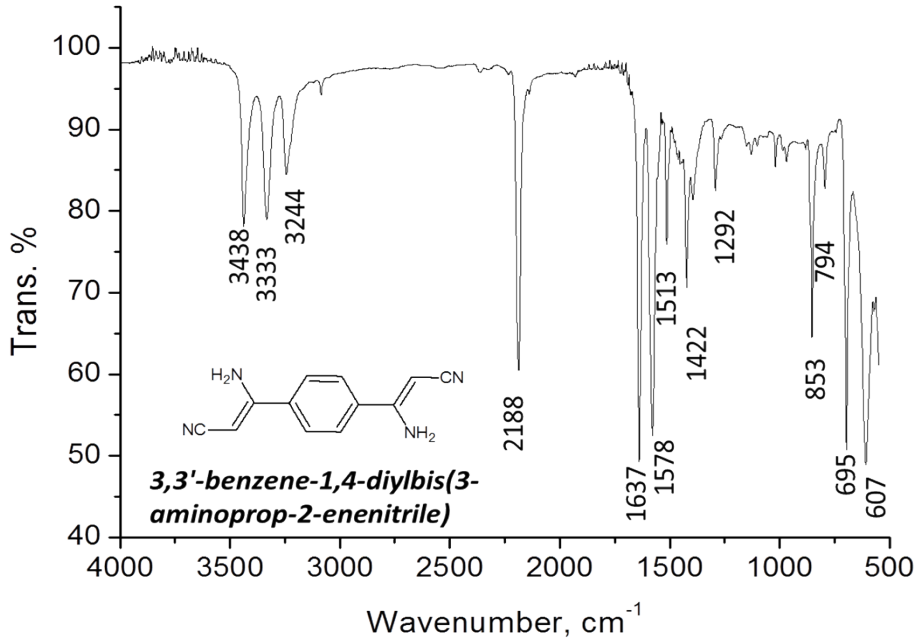

Figure S2. FTIR spectrum of 3,3'-benzene-1,4-diylbis(3-aminoprop-2-enenitrile).

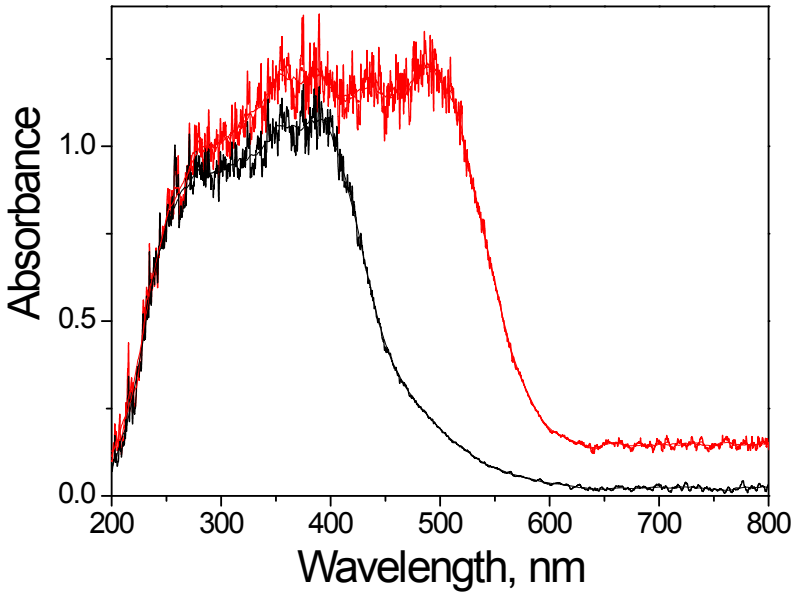

Figure S3. Solid-state UV-vis spectra of protonated and deprotonated PMF materials (black: protonated; red: deprotonated). The protonated PMFs are yellow turns red on deprotonation with OH^-. This protonation/deprotonation reaction is reversible.

(2) **Gas Adsorption Studies**

Nitrogen Adsorption

Isotherms for nitrogen adsorption and desorption at 77 K on PMF-NOTT-1 and PMF-NOTT-2 (black squares: adsorption; open squares: desorption) and DFT/Monte-Carlo pore size distributions (slit pore model; liquid N_2 density: 0.808 g cm^{-3}) are shown in Figures S4 and S5, respectively.

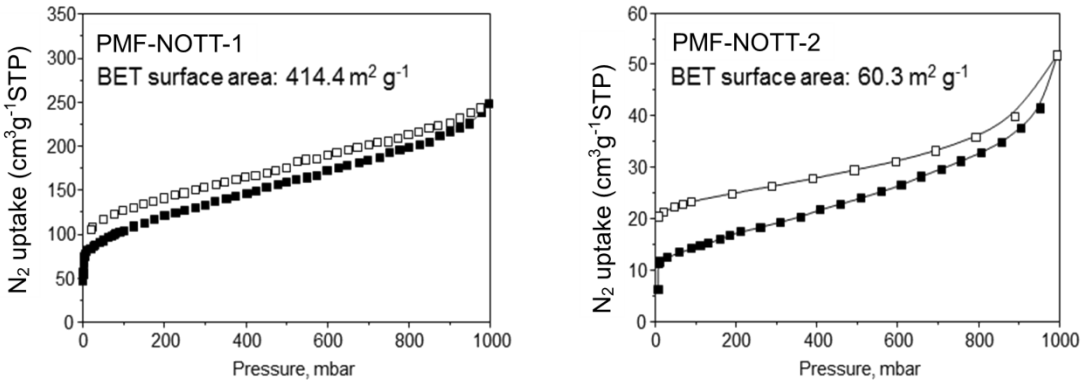

Figure S4. Isotherms of nitrogen adsorption and desorption on PMF-NOTT-1 and PMF-NOTT-2 at 77 K (black squares: adsorption; open squares: desorption).

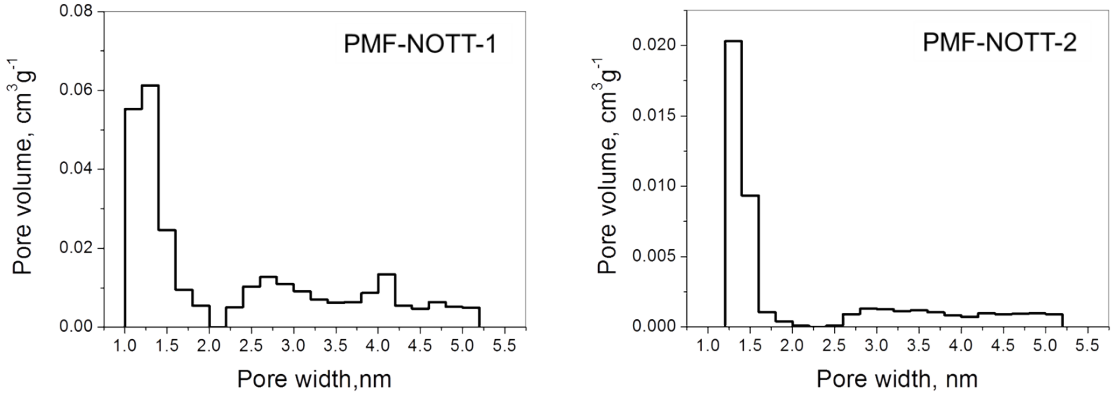

Figure S5. DFT/Monte-Carlo pore size distributions (slit pore model; liquid N_2 density: 0.808 g cm^{-3}).

Dubinin-Radushkevich (D-R) Graphs for CO_2 adsorption

The D-R plots of CO_2 adsorption isotherms on PMF-NOTT-1 and PMF-NOTT-2 are given in Figure S6. It is evident that the D-R graphs overlap when plotted on a relative pressure (p/p^0) basis.

a)

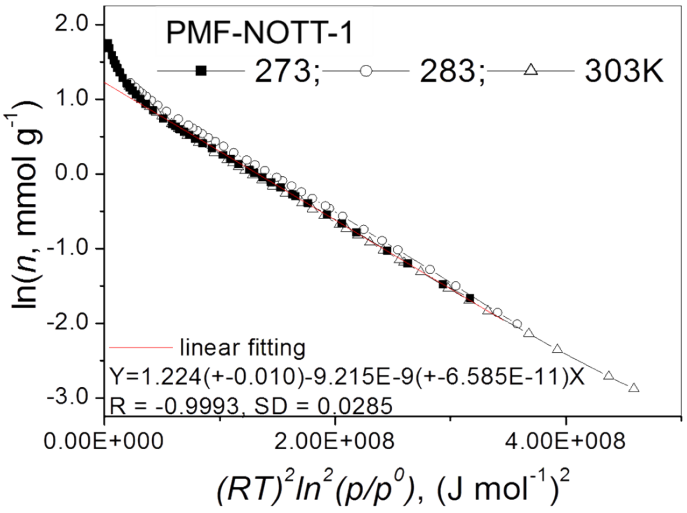

b)

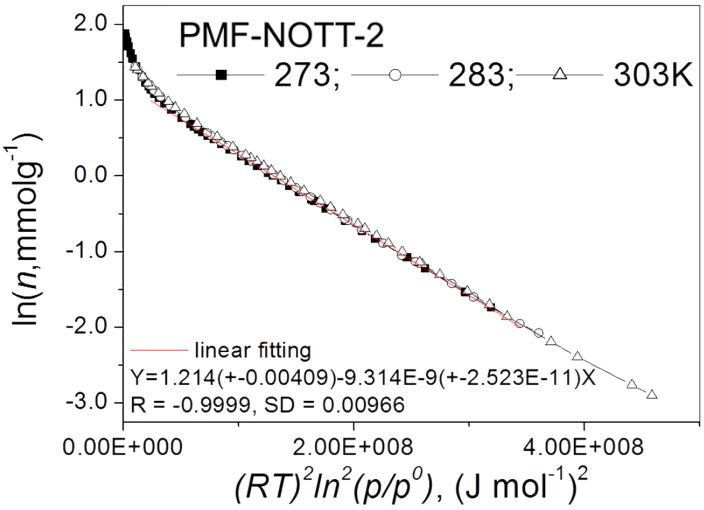

Figure S6. Dubinin-Radushkevich graphs of CO_2 adsorption isotherms at 273-303 K on a) PMF-NOTT-1 and b) PMF-NOTT-2.

Virial Equation Analysis

a)

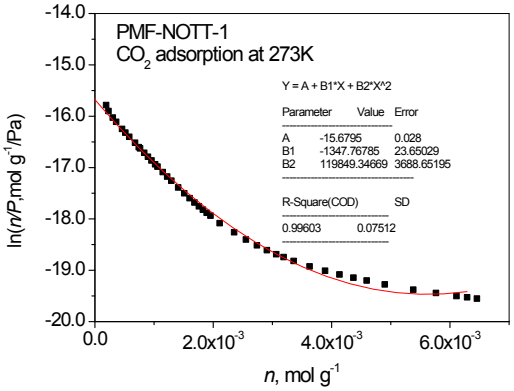

b)

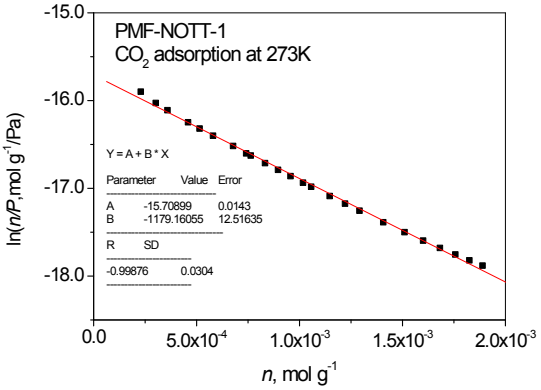

c)

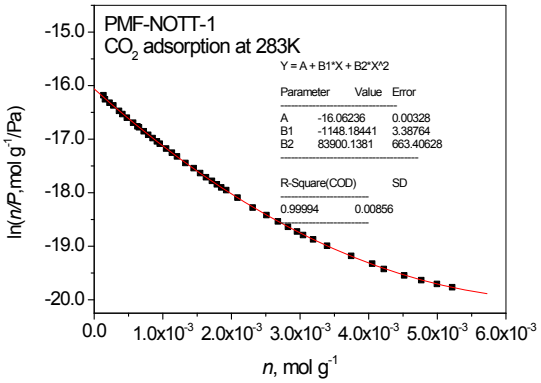

d)

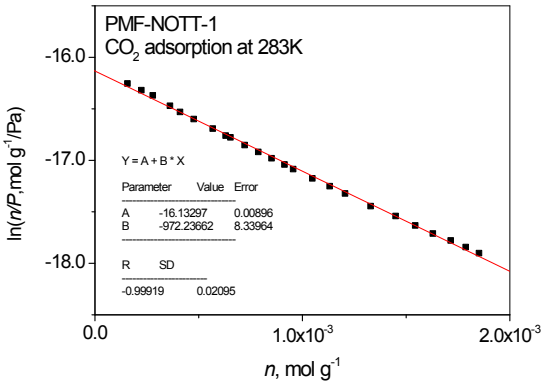

e)

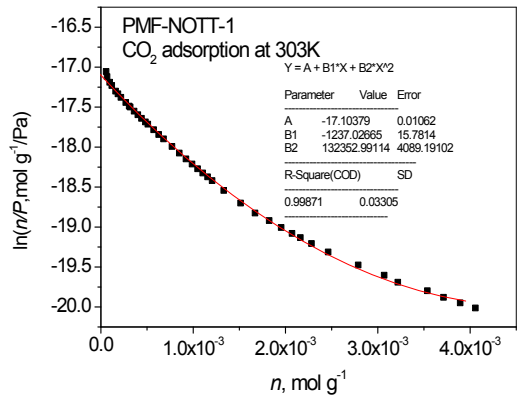

f)

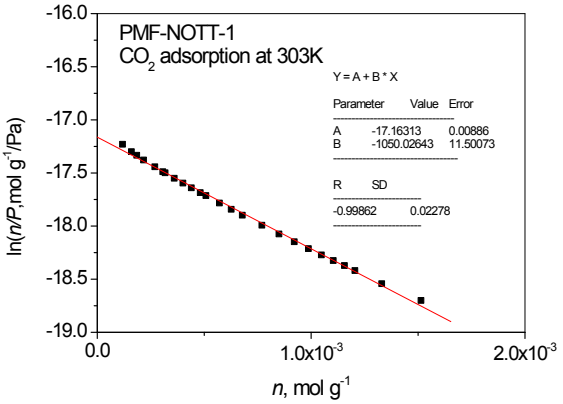

g)

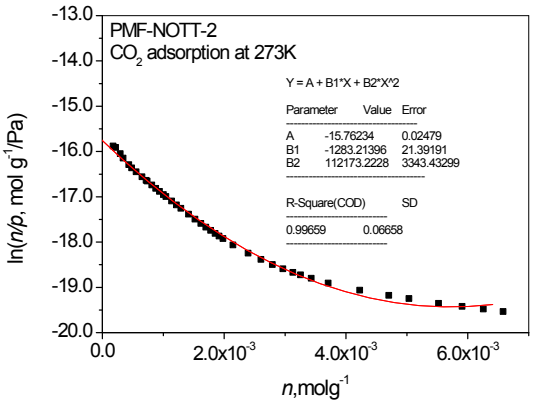
PMF-NOTT-2
CO2 adsorption at 273K
Y = A + B1*X + B2*X^2
Parameter Value Error
A -15.76234 0.02479
B1 -1283.21396 21.39191
B2 112173.2228 3343.43299
R-Square(COD) SD
0.99659 0.06658
ln(n/p, mol g-1/Pa)
n,molg-1

h)

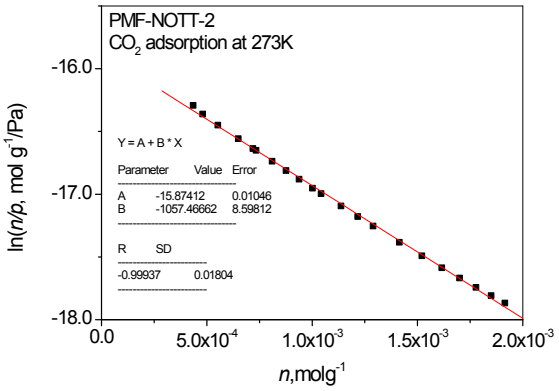
PMF-NOTT-2
CO2 adsorption at 273K
Y = A + B * X
Parameter Value Error
A -15.87412 0.01046
B -1057.46662 8.59812
R SD
-0.99937 0.01804
ln(n/p, mol g-1/Pa)
n,molg-1

i)

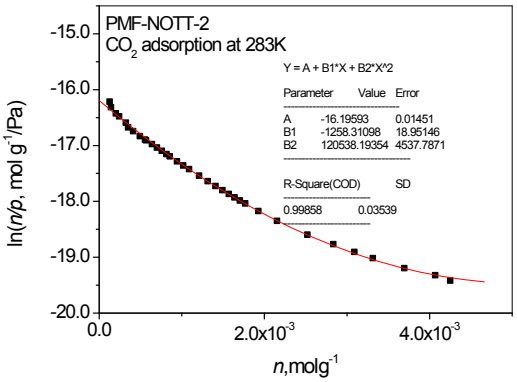
PMF-NOTT-2
CO2 adsorption at 283K
Y = A + B1*X + B2*X^2
Parameter Value Error
A -16.19593 0.01451
B1 -1258.31098 18.95146
B2 120538.19354 4537.7871
R-Square(COD) SD
0.99858 0.03539
ln(n/p, mol g-1/Pa)
n,molg-1

j)

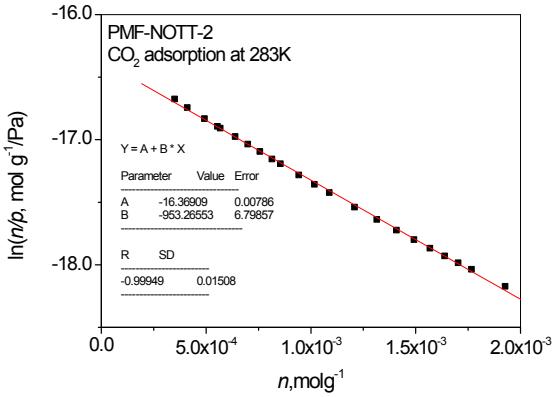
PMF-NOTT-2
CO2 adsorption at 283K
Y = A + B * X
Parameter Value Error
A -16.36909 0.00786
B -953.26553 6.79857
R SD
-0.99949 0.01508
ln(n/p, mol g-1/Pa)
n,molg-1

k)

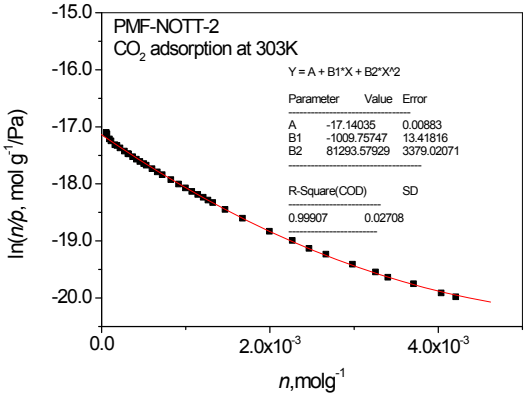
PMF-NOTT-2
CO2 adsorption at 303K
Y = A + B1*X + B2*X^2
Parameter Value Error
A -17.14035 0.00883
B1 -1009.75747 13.41816
B2 81293.57929 3379.02071
R-Square(COD) SD
0.99907 0.02708
ln(n/p, mol g-1/Pa)
n,molg-1

l)

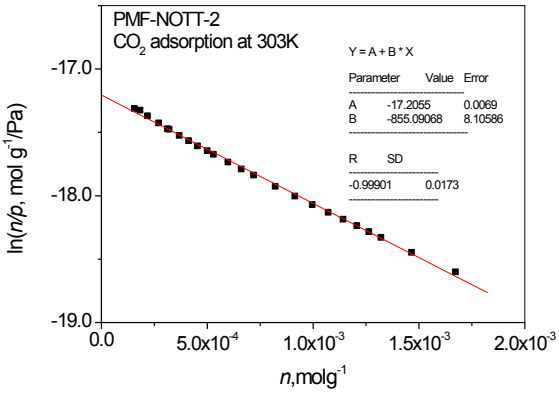
PMF-NOTT-2
CO2 adsorption at 303K
Y = A + B * X
Parameter Value Error
A -17.2055 0.0069
B -855.09068 8.10586
R SD
-0.99901 0.0173
ln(n/p, mol g-1/Pa)
n,molg-1

Figure S7. Virial graphs (polynomial: ln $(n/P) = A_0 + A_1n + A_2n^2$ and linear: ln $(n/P) = A_0 + A_1n$) for CO_2 adsorption isotherms of PMF-NOTT-1 and PMF-NOTT-2 at 273, 283 and 303 K. a) PMF-NOTT-1 (273 K) (Polynomial Equation), b) PMF-NOTT-1 (273 K) (Linear Equation), c) PMF-NOTT-1 (283 K) (Polynomial Equation), d) PMF-NOTT-1 (283 K) (Linear Equation), e) PMF-NOTT-1 (303 K) (Polynomial Equation), f) PMF-NOTT-1 (303 K) (Linear Equation), g) PMF-NOTT-2 (273 K) (Polynomial Equation), h) PMF-NOTT-2 (273 K), (Linear Equation) i) PMF-NOTT-2 (283 K) (Polynomial Equation), j) PMF-NOTT-2 (283 K) (Linear Equation), k) PMF-NOTT-2 (303 K) (Polynomial Equation), l) PMF-NOTT-2 (303 K) (Linear Equation).

The isosteric adsorption heat at zero coverage ($q^{st,0}$) was calculated from the gradient of plotting A_0 against $1/T$ i.e. $\partial A_0/\partial(1/T) = q^{st,0}/R$ (R = 8.314 J K^{-1} mol^{-1}).

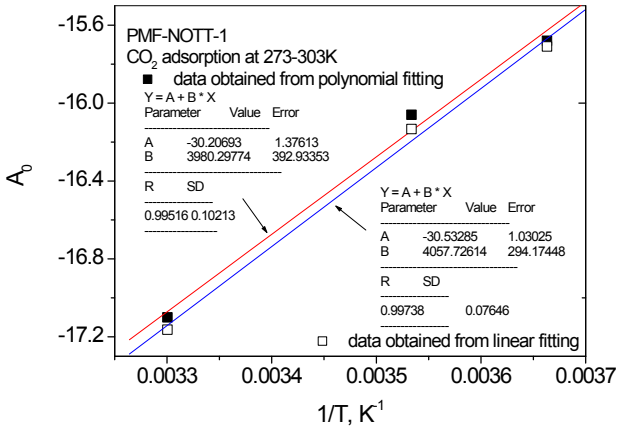

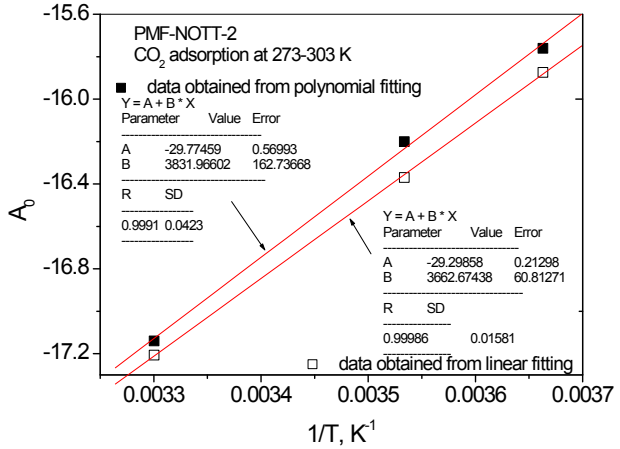

Figure S8. Variation of virial parameter A_0 with 1/T for a) PMF-NOTT-1 and b) PMF-NOTT-2. The isosteric heat ($q^{st,0}$) of adsorption at zero surface coverage was calculated from the gradient of the straight line. The polynomial fitting of ln $(n/p) \sim n$ gives values for PMF-NOTT-1 of 33.09 ± 3.26 kJ mol^{-1} and for PMF-NOTT-2 of 31.86 ± 1.35 kJ mol^{-1}; as a comparison, linear fitting gives PMF-NOTT-1: 33.74 ± 2.44 kJ mol^{-1}, PMF-NOTT-2: 30.45 ± 0.51 kJ mol^{-1}.

a) b)

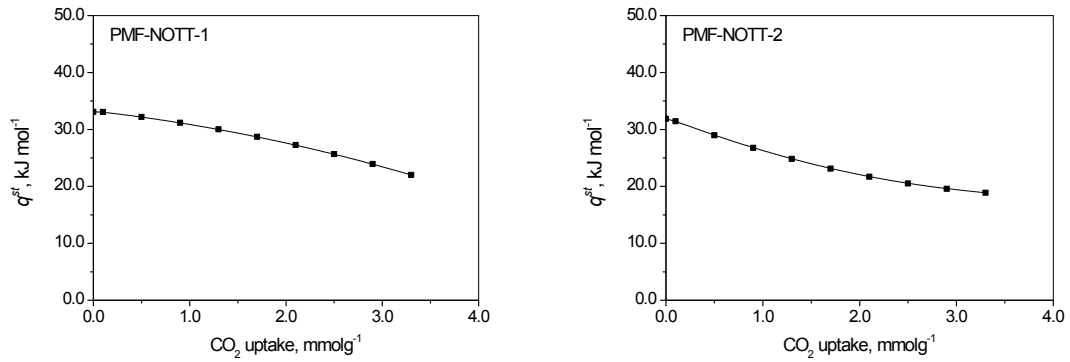

Figure S9. Variation of isosteric heat of adsorption (q^{st}) with amount of CO_2 adsorbed a) PMF-NOTT-1 and b) PMF-NOTT-2.

a) b)

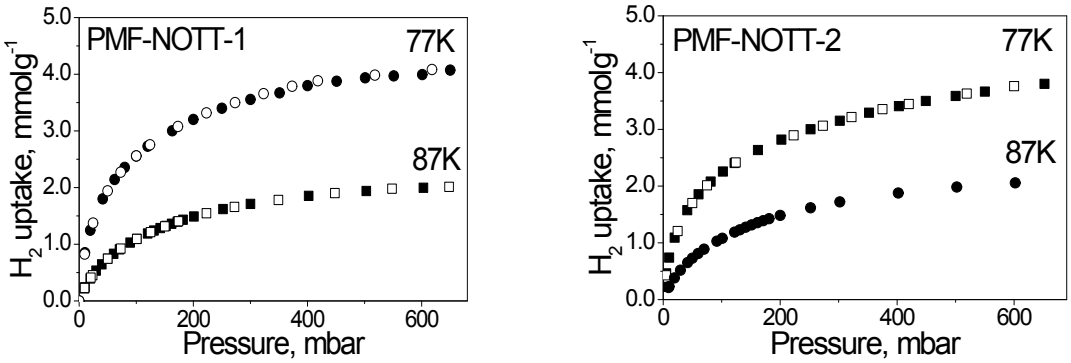

Figure S10. Adsorption isotherms for H_2 in a) PFM-NOTT-1 and b) PFM-NOTT-2 at 77 and 87 K (closed symbols: adsorption; open symbols: desorption).

a) b)

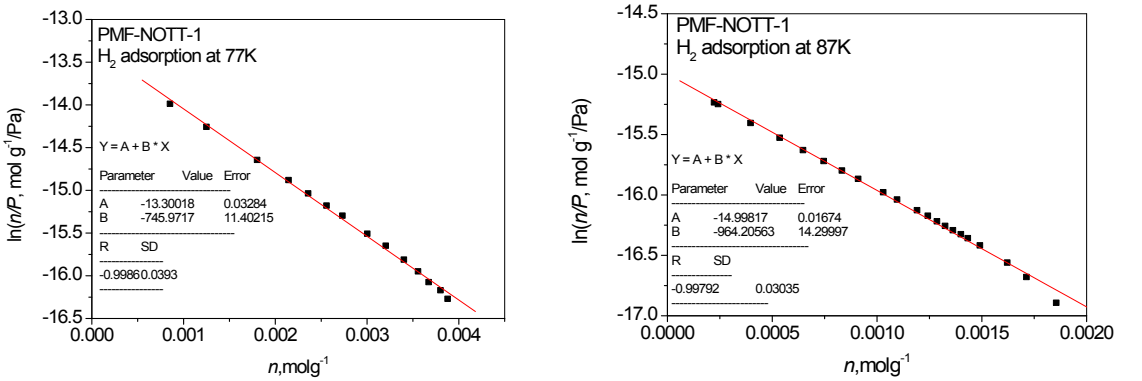

c) d)

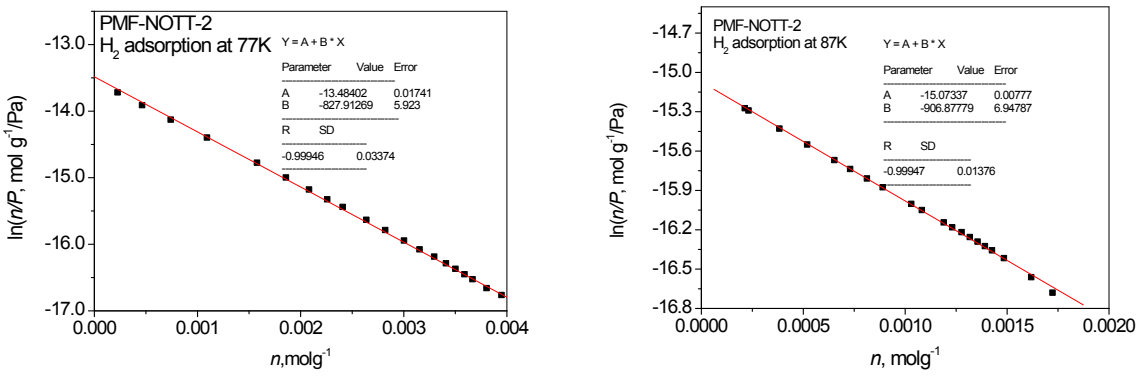

Figure S11. Virial graphs for equation ln $(n/P) = A_0 + A_1 n$ for H_2 adsorption for a) PMF-NOTT-1 (77 K) b) PMF-NOTT-1 (87 K), c) PMF-NOTT-2 (77 K), d) PMF-NOTT-2 (87 K)

The isosteric heat of adsorption at zero coverage ($q^{st,0}$) was calculated from the gradient of the graph of A_0 against $1/T$ i.e. $\partial A_0/\partial(1/T) = q^{st,0}/R$ (R = 8.314 $JK^{-1}mol^{-1}$) (for PMF-NOTT-1: $q^{st,0}$ = 9.46 kJ mol^{-1} ; for PMF-NOTT-2: $q^{st,0}$ = 8.85 kJ mol^{-1}).

(3) Catalysis Studies

Table S1. Data for different runs of the Knoevenagel condensation between aldehydes and malonitriles using PMF-NOTT-1 and PMF-NOTT-2 catalysts. [a]

Run	Entry	Aldehyde	Catalyst	Time (h)	Conversion (%)[b]	Selectivity (%)[b]
1	**7a**	Benzaldehyde	PMF-NOTT-1	54	68	98
2	**7a**	Benzaldehyde	PMF-NOTT-1[c]	54	66	98
3	**7a**	Benzaldehyde	PMF-NOTT-1[d]	54	63	98
4	**7a**	Benzaldehyde	PMF-NOTT-2	54	36	98
5	**7b**	4-chlorobenzaldehyde	PMF-NOTT-1	52	64	97[e]
6	**7c**	4-cyanobenzaldehyde	PMF-NOTT-1	52	54	98[e]
7	**7d**	4-methylbenzaldehyde	PMF-NOTT-1	52	93	97[e]

[a] Reaction conditions: aldehyde (1 mmol), malonitrile (1 mmol), toluene (4 mL), catalyst (20 mg), 110 °C. [b] Determined by GC. [c] First reuse; [d] Second reuse; [e] 2 % of corresponding acid was observed.

(4) Scanning Electron Micrographs

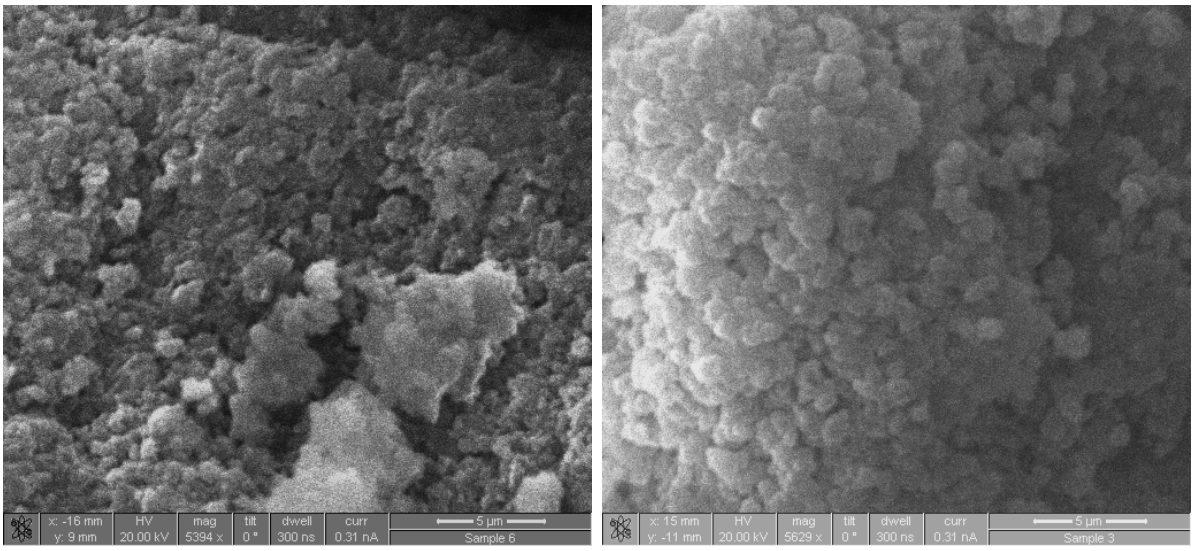

(PMF- NOTT-1) (PMF-NOTT-2)

Figure S12. SEM images show the spherical morphology of PMF-NOTT-1 and PMF-NOTT-2.